Examining the Robustness and Concentration Dependency of PFAS Air-Water and NAPL-Water Interfacial Adsorption Coefficients

Mark L Brusseau*

Environmental Science Department (Home) and Hydrology & Atmospheric Sciences Department (Joint)

University of Arizona

Prepared for review in:

Water Research

September 2020

Revised: December 15, 2020

^{*}Brusseau@arizona.edu

1 Abstract

2

3

4

5

6

7

8

9

10

11

12

13

14

15

16

17

18

19

20

21

Determining robust values for the air-water or NAPL-water interfacial adsorption coefficient, K_{IA}, is key to characterizing and modeling PFAS transport and fate in several environmental systems. Direct, high-resolution measurements of surfactant adsorption at the fluidfluid interface were aggregated from the literature. This data set was used to examine the accuracy and applicability of Γ and K_{IA} measurements determined for three PFAS from transport experiments and surface-tension data. The transport-measured Γ and K_{IA} data were observed to be fully consistent with the directly-measured data. Specifically, Γ values for the two methods were entirely coincident in the region of overlapping concentrations, which spanned ~4 orders-ofmagnitude. Furthermore, the two data sets adhered to an identical Γ -C profile. These results conclusively demonstrate the accuracy of the transport-measured values. Γ and K_{IA} values determined from the application of the Gibbs adsorption equation to measured surface-tension data were fully consistent with the directly-measured and transport-measured data sets, demonstrating their applicability for representing PFAS transport in environmental systems. The directlymeasured data were used to examine the concentration dependency of K_{IA} values, absent the potential confounding effects associated with the use of surface-tension or transport-measured data. The directly-measured data clearly demonstrate that K_{IA} attains a constant, maximum limit at lower concentrations. Two separate analyses of the transport-measured data both produced observations of constant K_{IA} values at lower concentrations, consistent with the directly-measured data. These outcomes are discussed in terms of surface activities, relative surface coverages, and critical concentrations.

22

Keywords: PFOS; PFOA; perfluoroalkyl substances; transport; leaching; retention

23

1. Introduction

Per- and poly-fluoroalkyl substances (PFAS) are now recognized as emerging contaminants of critical concern due to their widespread presence and long-term persistence in the environment (e.g., Ahrens, 2011; Cousins et al., 2016; Xiao, 2017; Hatton et al., 2018; Brusseau et al., 2020). As such, there is great interest in characterizing and modeling their transport and fate in environmental systems. Most PFAS have a propensity for adsorbing at interfaces. Numerous studies have been conducted for example to investigate PFAS interactions at aqueous-solid interfaces. More recently, adsorption of PFAS at fluid-fluid, particularly air-water, interfaces has become a focus of research.

As discussed by Brusseau (2019a), there are at least four major scenarios for which fluid-fluid interfacial adsorption may be critically important for the transport and fate of PFAS in the environment. Recent research has demonstrated that soils are a primary reservoir of PFAS (e.g., Anderson et al., 2019; Brusseau et al., 2020), and has illustrated the potential for PFAS-contaminated soil to serve as a source of groundwater contamination (e.g., Xiao et al., 2015; Weber et al., 2017; Dauchy et al., 2019; Høisæter et al., 2019; Guo et al., 2020). The results of miscible-displacement column experiments, mathematical modeling, and chemometric analysis have confirmed the significance of air-water interfacial adsorption for PFAS transport in unsaturated porous media (Brusseau, 2018; Lyu et al., 2018; Brusseau, 2019b, 2020; Brusseau et al., 2019a; Guo et al., 2020; Lyu and Brusseau, 2020; Lyu et al., 2020; Yan et al., 2020; Li et al., 2021). PFAS and organic immiscible liquids (NAPL) may co-exist in some source zones (e.g., Moody et al., 2003; McGuire et al., 2014), and adsorption at NAPL-water interfaces may affect the migration of PFAS in such cases (McKenzie et al., 2016; Brusseau, 2018; Brusseau et al., 2019a). For a third scenario, water droplets and hydrated aerosols in the atmosphere provide air-water interface that

may serve as retention domains for PFAS (e.g., Rontu and Vaida, 2007; McMurdo et al., 2008; Psillakis et al., 2009; Reth et al., 2011), which may be significant considering that certain PFAS undergo extensive atmospheric transport (e.g., Simcik, 2005; Prevedouros et al., 2006; Ahrens et al., 2011; Rauert et al., 2018). Finally, air-water interfaces are relevant in several treatment and remediation processes (e.g., Vecitis et al., 2008; Meng et al., 2014; Dai et al., 2019).

48

49

50

51

52

53

54

55

56

57

58

59

60

61

62

63

64

65

66

67

68

69

70

All of these scenarios require knowledge of the interfacial adsorption behavior of PFAS for accurate characterization, modeling, and design. Determining robust values for the air-water or NAPL-water interfacial adsorption coefficient, K_{IA}, is key to characterizing and modeling PFAS transport and fate in these environmental systems. Therefore, there is great interest in the measurement of K_{IA} values and in their functional dependency on system conditions. Of particular concern is the determination of KIA values that are representative of the dynamic conditions relevant to transport in the environment. The standard method for determining K_{IA} values is to measure surface/interfacial tension as a function of aqueous concentration and to apply the Gibbs adsorption equation. This method is a convenient and easily accessible approach for characterizing fluid-fluid interfacial adsorption and determining K_{IA} values. A critical question to address is if this approach produces K_{IA} values that are applicable to PFAS transport in dynamic environmental systems. Another issue of particular import for PFAS transport in the environment is the concentration dependency of K_{IA} values, given that environmentally relevant concentrations span many orders of magnitude. Lyu et al. (2018) presented the first comparison of transport-measured and surface-tension based KIA values and examination of their concentration dependency. The present study represents an in-depth follow-up investigation of these issues.

The objectives of this study are three-fold. Transport experiments and surface-tension measurements both produce indirect determinations of fluid-fluid interfacial adsorption and

associated K_{IA} values. Hence, the first objective is to examine the robustness of these methods through a comparison to data generated by direct measurements of fluid-fluid interfacial adsorption. The results of multiple studies that have used advanced, high-resolution methods to directly measure adsorbed quantities of surfactant at air-water and NAPL-water interfaces are aggregated from the literature to generate a gold-standard reference data set. This data set provides a robust benchmark for evaluating the accuracy of measurements based on transport experiments, surface-tension measurements, and other methods. It also provides a direct means of examining the concentration dependency of KIA values. For the second objective, the largest set of KIA data obtained to date from miscible-displacement transport experiments is aggregated and analyzed to determine their robustness and concentration dependency. A potential source of uncertainty in determining K_{IA} values from transport experiments is the need to quantify the magnitude of airwater or NAPL-water interface. Novel approaches are employed herein that minimize or eliminate this potential uncertainty. The third objective entails examining the robustness of KIA values determined from surface-tension data and their relevancy for transport conditions by comparing them to directly-measured and transport-based values. Application of the Gibbs equation to surface-tension data is often accompanied by an assumption of a specific isotherm model, which introduces a source of uncertainty. An alternative approach is used herein that eliminates the need for isotherm-model specification and the associated uncertainty. In total, this study provides the first comprehensive investigation of the accuracy and robustness of K_{IA} values relevant for PFAS transport in environmental systems.

91

71

72

73

74

75

76

77

78

79

80

81

82

83

84

85

86

87

88

89

90

92

93

2. Theory

The amount of PFAS or any substance adsorbed at a fluid-fluid interface, often referred to as surface excess, is defined as Γ (mol/cm²). The relationship between surface excess and the bulk solution concentration (C, mol/cm³) defines the K_{IA} :

98
$$K_{IA} = \Gamma/C \qquad (1)$$

where K_{IA} has units of cm. The Gibbs adsorption equation provides a thermodynamically based relationship between surface tension and surface excess:

$$\Gamma = \frac{-1}{\text{xRT}} \frac{\partial \gamma}{\partial lnC} = \frac{-C}{\text{xRT}} \frac{\partial \gamma}{\partial C}$$
 (2)

where γ is the surface or interfacial tension (dyn/cm or mN/m), T is temperature (°K), R is the universal gas constant (dyne-cm/mol °K), and x in simplified terms is a coefficient equal to 1 for systems with nonionic surfactants or ionic surfactants with excess electrolyte in solution, and equal to 2 for systems with ionic surfactants without excess electrolyte (e.g., deionized water). Combining equations 1 and 2 produces:

$$K_{IA} = \frac{-1}{\text{xRT C}} \frac{\partial \gamma}{\partial lnC} = \frac{-1}{\text{xRT}} \frac{\partial \gamma}{\partial C}$$
 (3)

Equations 2 and 3 are greatly significant in that their application allows the determination of Γ and K_{IA} values, respectively, from measured surface/interfacial-tension data. For convenience, Γ and K_{IA} values determined in this manner will be referred to henceforth as "ST-Gibbs" values. It is important to note that such values are thermodynamic-based measurements derived, albeit indirectly, from measured surface or interfacial tensions.

It is widely accepted, standard practice in surfactant and surface science fields to apply the Gibbs equation to measured surface/interfacial-tension data to determine surface excess. As noted in the Introduction, a critical question to address is if Γ and K_{IA} values determined from ST-Gibbs

are applicable for the transport of PFAS in dynamic environmental systems. The first step in such an assessment is to consider and review the inherent validity of Γ and K_{IA} values determined with ST-Gibbs. Questions regarding the validity of ST-Gibbs measurements are fundamentally a question of the validity of the Gibbs equation or, more accurately as will be discussed below, its application.

Numerous investigators have demonstrated via detailed treatments that the Gibbs adsorption equation is based on rigorous thermodynamic principles (e.g., Davies and Rideal, 1962; Defay et al., 1966; Chattoraj and Birdi, 1984). This work continues, as illustrated by a recent treatment that demonstrated via thermodynamic principles that both zero-volume and finite-volume assumptions for the Gibbs dividing surface produce identical results for the Gibbs adsorption equation, confirming the thermodynamic generality and rigor of the equation (Radke, 2015). Hence, there is no question of the inherent validity of the Gibbs adsorption equation in and of itself. Therefore, questions of its validity are in reality questions of its application, particularly with respect to the use of surface/interfacial tension data to determine Γ (and thus K_{IA}).

The quest to demonstrate experimentally the validity of the Gibbs adsorption equation and its application has been ongoing for decades. The gold-standard approach is to employ an experimental method that can directly measure the amount of adsorbate present at the fluid-fluid interface, and then to compare the independently measured adsorption isotherm to the one determined from ST-Gibbs. Numerous methods have been employed to successfully accomplish this, including physical collection of the surface excess using microtome or bubble-generation systems, radiotracer measurement, optical methods, various spectroscopic methods, and neutron reflectometry. Davies and Rideal (1961) and Defay et al. (1966) provide overviews of the many initial attempts conducted in the early-mid 1900's to use independent measurements to validate

application of the Gibbs equation. Many of the earliest attempts employed physical means such as microtomes or bubble generation to physically collect the surface excess for subsequent quantification. For example, good correspondence was observed between surface excess measured with a microtome method versus ST-Gibbs (Snavely et al., 1962). Several investigators have used radiolabeled surfactants to provide direct quantification of the surface excess and shown consistency with ST-Gibbs (e.g., Tajima et al., 1970; Muramatsu et al., 1973). More recently, neutron reflectometry has become a standard method for the direct measurement of adsorbed surfactant at air-water interfaces.

139

140

141

142

143

144

145

146

147

148

149

150

151

152

153

154

155

156

157

158

159

160

161

Many of the applications of neutron reflectometry (NR) for direct measurement of surfactant adsorption at the air-water interface have used PFAS as the test surfactant. Simister et al. (1992) and Downes et al. (1995) both reported that Γ_{max} values measured directly with NR compared well to those determined with ST-Gibbs for NH4-PFOA. An et al. (1996) used NR to measure isotherms for Cs-PFOA, Na-PFOA, and H-PFOA in the absence and presence of excess electrolyte. These directly measured isotherms were compared to those determined with ST-Gibbs. They showed that the presence of impurities in solution caused a disparity between the two sets of isotherms for the system without excess electrolyte. However, the isotherms matched well when the impurities were removed. They also matched well for the isotherms measured in solutions containing excess electrolyte, the addition of which ameliorates the impacts of impurities. Downer-Eastoe et al. reported similar results for Na-perfluorononanoate (PFNA) and Na-9-H perfluorononanoate in a series of papers. Downer et al. (1999a) observed that isotherms determined with ST-Gibbs deviated from those measured with NR, and attributed this disparity to the presence of impurities. This was confirmed in follow-up studies, wherein it was reported that the two sets of isotherms matched well when all sources of impurities were removed (Downer et al., 1999b;

Eastoe et al., 2000). Similarly, the ST-Gibbs based isotherm matched very well to the isotherm measured directly with NR for NH₄-PFNA (Sekine et al., 2004).

In addition to the results reported in the preceding paragraph for the anionic perfluoroalkyls PFOA and PFNA, consistency between NR-measured and ST-Gibbs-measured isotherms has been demonstrated for other PFAS. These include anionic dual-chain polyfluoroalkyl sulfosuccinates (Downer et al., 1999b; Eastoe et al., 2000), nonionic perfluoroalkyl triethyleneoxide methyl ethers (Eastoe et al., 2001), nonionic fluorinated ethylene oxides (Richards et al., 2003; Eastoe et al., 2006), and a nonionic fluorotelomer (Dupont et al., 2003). Consistency between NR and ST-Gibbs isotherms has also been reported for a range of hydrocarbon surfactants, including anionics, cationics, nonionics, and zwitterionics (e.g., Lu et al., 1993; Hines et al., 1997; Nave et al., 2000).

Malec et al. (2004) used horizontal-touch voltammetry (HTV) and Brewster angle microscopy as two independent methods to directly measure the air-water interfacial adsorption isotherm for a nonionic hydrocarbon surfactant (C8Tempo). The isotherm determined from ST-Gibbs compared very well to the two directly measured isotherms. This is shown in the reproduced data presented in Figure 1. It is noted that the Langmuir isotherm provides an excellent fit to the measured data sets over the entire concentration range.

In summary, it is indisputable that the Gibbs adsorption equation is fundamentally valid. Furthermore, the research highlighted above, in addition to other works, has conclusively demonstrated that application of the Gibbs adsorption equation to surface/interfacial tension data produces correct measurements of surface excess, validating the standard approach. Hence, any discrepancies observed when employing this approach are not an issue of the inherent validity of the Gibbs equation itself or its fundamental application, but rather the result of experimental limitations related to impurities, measurement error, or other issues (e.g., An et al., 1996;

Mukherjee et al., 2013; Martínez-Balbuena et al., 2017). As a corollary, K_{IA} values determined from ST-Gibbs must therefore also be valid in principle. It is particularly noteworthy that many of the experiment-based demonstrations of validity discussed above employed various PFAS. Hence, there is no readily apparent reason that Γ and K_{IA} values determined from ST-Gibbs should not be valid in general for the adsorption of PFAS at air-water or NAPL-water interfaces. The relevant question then becomes, if such values are applicable for the dynamic conditions of PFAS transport in environmental systems.

3. Methods

3.1 Data Sets

Published transport and surface-tension data sets are used for this study. Brusseau and colleagues reported the first PFAS K_{IA} values determined from unsaturated-flow miscible-displacement transport experiments (Lyu et al., 2018; Brusseau et al., 2019a; Brusseau, 2020; Lyu and Brusseau, 2020; Yan et al., 2020). The raw data were reprocessed and aggregated as described in the Supplemental Information (SI) file (section SI-1). Two recent studies of PFOA transport in unsaturated sand conducted by another research group (Lyu et al., 2020; Li et al., 2021) are available for comparison to the work of Brusseau and colleagues. These are described in section SI-1 of the SI. Surface-tension data sets are also reported in the source studies. Additional PFOA surface-tension measurements were conducted for this study as described in the SI (SI-2). Several studies reporting direct measurements of the adsorption of surfactants at the air-water and NAPL-water interfaces were retrieved from the literature. These are listed in Table SI-1 in the SI file.

Transport-measured data are presented for three PFAS (PFOA, PFOS, APMO) and for one hydrocarbon surfactant (SdDBS). Note that both air-water and NAPL-water data are available for

PFOS from the study of Brusseau et al. (2019a), with decane as the NAPL. Directly-measured data are presented for three PFAS (PFOA, PFNA, C6F13PEO) and for several common hydrocarbon surfactants, including SDS. The acronyms are defined in Table SI-2 in the SI.

3.2 Miscible-Displacement Transport Data Analysis

The retardation factor, R, for aqueous-phase transport of an adsorbing solute under waterunsaturated conditions is defined as (e.g., Kim et al., 1997; Brusseau et al., 2007):

$$R = 1 + K_d \rho_b / \theta_w + K_{IA} A_{IA} / \theta_w$$
 (4)

where K_d is the solid-phase sorption coefficient (cm³/g), ρ_b is porous-medium bulk density (g/cm³), θ_w is volumetric water content (-), and A_{IA} is the specific air-water or NAPL-water interfacial area (cm²/cm³). Note that the latter term represents the amount of fluid-fluid interfacial area normalized by the volume of the porous medium. The R in equation 4 comprises contributions from all sources of retention. The contribution associated with adsorption at the fluid-fluid interface is:

221
$$K_{IA}^{0} = K_{IA}A_{IA}/\theta_{w}$$
 (5)

where $K_{IA}{}^0$ is the nondimensional term representing the magnitude of fluid-fluid interface retention, which can be considered a normalized K_{IA} .

Details of how R and $K_{IA}{}^0$ are quantified from the breakthrough curves generated from transport experiments are provided in the SI (section SI-1). The description of how measured surface-tension data are used in conjunction with the Gibbs equation to determine Γ and K_{IA} values is also provided in the SI (section SI-2). Discussion of potential sources of uncertainty for determination of the measurements is provided in relevant sections of the SI and in section 4.3 of the Results and Discussion.

4. Results and Discussion

231

232

233

234

235

236

237

238

239

240

241

242

243

244

245

246

247

248

249

250

251

252

253

4.1 Data Comparisons and Concentration Scaling

Γ and K_{IA} values measured for multiple PFAS and hydrocarbon surfactants in different ionic-strength solutions are compared in this study as a function of aqueous concentrations. The relevant concentrations for such comparisons are not the actual values but rather the concentrations relative to the respective surface activities of each surfactant-solution system. Hence, the aqueous concentrations are scaled to account for the differences in surface activities of the different systems. One approach for scaling is to normalize the concentration by a reference concentration such as the critical micelle concentration (CMC). This approach has been used to scale both surface-tension and surface-excess data comprising different surfactants and different ionic strengths/compositions (e.g., Matuura et al., 1962; Hill et al., 2018). Other reference concentrations can also be used, such as the inflection point of the surface-tension curves (the point of maximum change in slope), which is a critical reference point (Brusseau, 2019a). For example, the inflection-point concentrations are approximately $3.3 \cdot 10^{-6}$ M, $3.3 \cdot 10^{-5}$ M, and $7.3 \cdot 10^{-5}$ M for PFOS, PFOA, and APMO, respectively. Another approach, based on mean ionic activity, has been used to scale systems comprising different ionic strengths (e.g., Miyajima et al., 1980; Fainerman et al., 2002). For example, Gurkov et al. (2005) used this approach to scale surfacecoverages calculated from surface-tension data for different surfactants, including both air-water and NAPL-water systems.

The concept of scaling to match surface activities is illustrated with two sets of surfacetension data, one reported by Lunkenheimer et al. (2015) for the C6-C11 series of Naperfluorocarboxylic acids and the other set reported by Brusseau and Van Glubt (2019) for Na-PFOA in different ionic-strength solutions (see Figure SI-1 in the SI). The C6-C11 data exhibit typical behavior wherein the PFAS with the longest chain has the greatest surface activity, and the surface activities decrease in sequence by chain length for the remaining PFAS (Figure SI-1A). The surface activity of PFOA is observed to be greater for higher ionic strength, as expected (Figure SI-1B). These data can be scaled as described above to account for the observed differences in surface activities.

The data scaled by the respective CMCs are presented in Figure SI-2A. The net result of scaling is that all 9 curves collapse into one master curve. This standard scaling procedure produces non-dimensional units for the normalized concentrations. This can be limiting in cases for which actual concentration units are desired. The data scaled by mean ionic activity are presented in Figure 2A-B. It is observed that this scaling approach produces a master curve for all of the PFOA (C8) data, including the different ionic strengths. However, this approach does not scale the different PFAS.

A novel scaling method is introduced in this study wherein concentrations are standardized to match the surface activity of a selected common or representative surfactant. PFOA is selected for the purposes of this study. For the example of PFOA, PFOS, and APMO, the net result of applying the alternative scaling with respect to PFOA is that the concentrations for PFOS and APMO are in effect multiplied by a scaling factor (S_f) of 10 and 0.45, respectively, based on their respective inflection-point reference values noted above. This produces scaled PFOS and APMO aqueous concentrations equivalent to those of PFOA in terms of similar surface activities. This scaling factor can be thought of as the relative surface-activity strength of a given surfactant compared to that of PFOA. For example, PFOS can be considered to have a 10-times greater surface activity than PFOA for a given non-scaled concentration. This approach allows the use of actual concentration units rather than normalized units. It is critical to note that this scaling

procedure does not change the inherent nature of the individual data sets. It only translates the curves along the x-axis to facilitate direct comparison. Specifically, the curve is translated rightward for $S_f>1$ and leftward for $S_f<1$. Thus, the actual nature of the relationships (e.g., the γ -C and Γ -C profiles) is preserved.

Application of this approach to the data sets presented in Figure SI-1 is shown in Figure SI-2C. All data sets collapse into one master curve. The respective scaling factors are reported in the figure caption. Scaled with respect to PFOA, it is observed that the scaling factors are larger than 1 for the PFAS with greater activities (longer chains), and less than 1 for those with weaker activities (shorter chains). Similarly, the scaling factors are greater than 1 for the two non-zero ionic-strength data sets.

4.2 Direct Measurements of Surfactant Adsorption at the Fluid-Fluid Interface

Several methods have been used to directly measure the adsorbed quantity of surfactant at the fluid-fluid interface (Γ), as previously discussed. Data sets collected from the literature for PFOA, PFNA, C6F13PEO, and 7 hydrocarbon surfactants are presented in Figure 2A. The specific data sets used in the figure, along with the respective Γ_{max} and scaling factors, are reported in Table SI-1. The measurements of Γ were extended to sufficient concentrations to attain maximum values. Therefore, the Γ_{max} values used for normalizing Γ were determined directly from the measured data. As noted above, the concentration scaling does not alter the Γ -C profiles of the individual data sets. To illustrate, the Γ -C data for SDS and SDBS plotted with actual, unscaled concentrations are reported in Figure 2B. Comparison of Figures 2A and 2B shows identical overall Γ -C profiles irrespective of scaling or no scaling. Together, these observations indicate that the normalization and scaling procedure did not introduce bias or uncertainty to the analysis.

The striking observation for Figure 2A is the consistency of all of the data sets. The measured data span more than 4.5 orders-of-magnitude in aqueous concentration. Of particular import, the measurements span from 100% down to \sim 0.6% relative surface coverage (Γ/Γ_{max}). In total, the data represent 11 different direct-measurement methods. Notably, data reported for SDS comprise 6 different measurement methods. Also of note is that three data sets are reported for NAPL-water systems, and that the data sets include measurements for solutions with ionic strengths of 0.1, 0.01, and \sim 0. These factors increase the degree of difficulty for and broaden the applicability of the comparative assessment.

One important point to address is the equilibrium conditions of the measurements. Neutron reflectometry is considered to provide equilibrium measures of surface excess (e.g., Eastoe et al., 2000, 2003). This has been confirmed for example by comparison of NR-measured isotherms to those measured by drop-volume tensiometry (e.g., Downer et al., 1999b; Eastoe et al., 2000, 2001, 2006; Nave et al., 2000; Dupont et al., 2003), the use of which ensures equilibrium is attained (e.g., Downer et al., 1999a; Eastoe et al., 2000, 2001). As noted above, 6 measurement methods were reported for SDS. The isotherms measured for SDS by the five other methods are consistent with the NR-measured isotherm. This indicates that the surface excesses measured by these other methods also represent equilibrium conditions.

It is critical to recognize that most of these measurements were obtained with advanced, high-resolution methods designed to directly characterize soft-matter surfaces and interfaces. These include the HTV, BAM, VSFS, NICISS, IRRAS, and NR methods. The other methods represent ingenious approaches for the physical collection (microtome, bubble generation, emulsion formation) or direct measurement (radiotracer) of surface excess. As such, these data represent the most accurate and robust direct measurements of surfactant adsorption at fluid-fluid

interfaces available. This data set serves as a gold-standard benchmark to which to compare measurements obtained with other methods.

Measured K_{IA} values can be determined from the data presented in Figure 2 by application of equation 1. Normalized K_{IA} values determined for the entire data set presented in Figure 2A are shown in Figure 3A. The non-scaled data set for air-water interfacial adsorption of SDS and SDBS determined from the data presented in Figure 2B is shown in Figure 3B. The K_{IA}-C functions are similar for scaled and non-scaled data, consistent with the adsorption isotherms. To our knowledge, these data represent the first reported K_{IA} values obtained from direct, high-resolution measurements of surfactant adsorption at air-water and NAPL-water interfaces.

It is clearly evident that the K_{IA} values asymptotically approach and eventually attain constant values at lower aqueous concentrations. The slope of the curve begins to decrease at a concentration >10⁻⁴ M and attains constancy at >10⁻⁵ M, after which it remains constant for more than 1.5 orders of magnitude change in concentration. These results clearly demonstrate that K_{IA} values for surfactant absorption at fluid-fluid interfaces are subject to a maximum upper limit at lower concentrations.

4.3 Transport-Measured Γ and K_{IA} values & Uncertainty Analysis

Example arrival fronts for transport of PFOA, PFOS, and APMO in the sand under unsaturated conditions are shown in Figure SI-3. The magnitude of retardation is observed to be greatest for PFOS, the PFAS with the longest chain and greatest surface activity, whereas APMO, which has the shortest chain and weakest surface activity, has the lowest magnitude of retardation. The contribution of solid-phase sorption to retardation is relatively low for all three PFAS. In addition, the magnitude of A_{IA} is similar for all three experiments because similar water saturations

were used. Hence, the observed significant differences in retardation are due to the relative magnitudes of air-water interfacial adsorption (i.e., K_{IA}) among the three PFAS.

There are four primary sources of uncertainty in the determination of K_{IA} (and Γ) values from transport experiments. The first two comprise measurement uncertainty associated with the transport experiments and the data-analysis methods used to determine retardation factors. These two sources are discussed in sections SI-3 and SI-4, respectively, of the SI. In summary, the methods used are demonstrably robust. The third source of uncertainty entails quantifying the contribution of solid-phase sorption for the determination of K_{IA}^0 with equation 4. Specification of A_{IA} for determination of K_{IA} from equation 5 is the fourth source of uncertainty. This latter step can be problematic in some cases, particularly for porous media that have not been sufficiently characterized. Inaccurate characterization of K_d and/or A_{IA} can be a source of uncertainty in generating representative K_{IA} and Γ values from transport experiments. These potential constraints are mitigated in this study through the use of highly characterized media.

The transport data used for this study were generated from experiments employing commercially available natural, well-sorted quartz sand. Several advantages accrue to using such a porous medium. First, this type of sand has been used in many transport studies conducted by numerous investigators and, as such, it serves as a reference natural porous medium. Second, our prior studies have shown that the sand has a very low magnitude of solid-phase sorption for the select PFAS used in the transport experiments. In addition, this sorption has been well characterized and quantified with both transport and batch-isotherm experiments (Van Glubt et al., 2021). As a result, the second term on the r.h.s. of equation 4 is both minor and well quantified, which means there is minimal associated uncertainty.

Another primary advantage of using the selected sand is that it is likely that more measurements of fluid-fluid interfacial areas have been reported for this particular medium than for any other porous medium. This provides a significant degree of certainty in determining relevant A_{IA} values for use in equation 5. In addition, this medium has an appreciable magnitude of air-water interfacial area. For the conditions of the experiments, the actual air-water interfacial areas range from ~3800 to 7500 cm² depending on the volume of the column employed. These large magnitudes provide great sensitivity to adsorption at the air-water interface, thereby enhancing the determination of robust K_{IA} values.

Multiple methods are available to measure A_{IA}, including various interfacial tracer techniques (e.g., Kim et al., 1997; Anwar et al., 2000; Schaefer et al., 2000; Brusseau et al., 2007, 2008; Araujo et al., 2015; Zhong et al., 2016), a gas-absorption/chemical-reaction method (Lyu et al., 2017), and high-resolution x-ray microtomography (XMT) (Brusseau et al., 2006, 2007; Araujo and Brusseau, 2019, 2020). These methods have been used in multiple studies to measure A_{IA} values for the sand used in this study. Measured values for the water saturations (~65%) relevant to the transport experiments are presented in Table SI-3. Inspection of Table SI-3 reveals that the measured fluid-fluid interfacial areas range from ~30 to ~100 cm⁻¹. The smallest values are those measured by XMT. A recent study demonstrated that XMT imaging provides very accurate and reproducible measurements of A_{IA}, including for the sand used in the present study (Araujo and Brusseau, 2020). A_{IA} values measured with XMT can therefore be considered as benchmark, baseline values for the sand. However, it is critical to note that the XMT values are smaller than actual transport-relevant values due to the fact that the XMT method does not measure interfacial area associated with microscopic surface roughness (Brusseau et al., 2007, 2008).

Interfacial tracer tests do characterize the contribution of microscopic surface roughness to fluid-fluid interfacial areas (e.g., Kim et al, 1999; Schaefer et al., 2000; Brusseau et al., 2007, 2008; Jiang et al., 2020). Interfacial areas measured with aqueous-phase interfacial tracer tests are anticipated to be the most relevant for PFAS transport scenarios, given the similarity of the experiment systems (Brusseau, 2019b, 2020). The tracer-based AIA values measured for saturations of ~0.65 are in the range of 70 to 100 cm⁻¹. The most relevant is the 87 cm⁻¹ value obtained for an air-water system with the miscible-displacement tracer method (row 3 in Table 1). The mean of the 6 tracer-test A_{IA} measurements (rows 3-8) is 85 cm⁻¹ (± 9.7 , 95% CI), which is close to the prior noted value. The uncertainty in AIA is 11% based on the 95% CI determined for the different interfacial tracer-test measurements. Interestingly, this value is very similar to the 9% measurement uncertainty reported by El Ouni et al. (2021) for the aqueous miscible-displacement interfacial-tracer method. Considering the existence of multiple, consistent independent AIA measurements for the sand, it can be concluded that there is a relatively high degree of confidence in the A_{IA} values employed and concomitantly that there is a correspondingly low degree of uncertainty in the determination of Γ and K_{IA} values from the transport experiments. The measurement uncertainty for θ_w (<1%) contributes minimally to Γ and K_{IA} uncertainty.

390

391

392

393

394

395

396

397

398

399

400

401

402

403

404

405

406

407

408

409

410

411

412

An additional transport-measured data set is obtained from experiments conducted for the transport of SdDBS in an unsaturated glass-bead medium (El Ouni et al., 2021). Air-water interfacial areas have been measured for this medium with high-resolution XMT (Araujo and Brusseau, 2020). Prior work has demonstrated that these glass beads do not have measurable surface roughness (Araujo and Brusseau, 2019). Therefore, the A_{IA} values measured by XMT can be used in equation 5 to determine K_{IA} for the transport experiments. These values have minimal uncertainty given the availability of the XMT-measured A_{IA} values.

The Γ values measured from the miscible-displacement transport experiments are presented in Figure 4. The relatively high degree of certainty associated with the column-measured data is illustrated in multiple ways. First, Γ values were measured for PFOA in 7 separate transport experiments for the data point labeled in the figure, and the 95% CI is within the size of the data symbol. Of particular note, these experiments not only included replicate tests but also tests conducted under different conditions (water content, pore-water velocity, solution conditions). Second, the measurement uncertainty for these values due to uncertainty in determination of A_{IA} (~11% as noted above) is equivalent to 1/3 larger than the size of the data symbols. Third, the Γ value determined from the independent PFOA transport study of Li et al. (2021) is consistent with the values determined from Lyu et al (2018). Fourth, the values determined for air-water and NAPL-water systems are consistent for PFOS. Finally, in aggregate, the transport-measured data span relative surface coverages from ~100% to ~0.01%. All of the values are approximately coincident along an identical Γ -C profile, illustrating great consistency amongst the data sets.

4.4 Comparison of Transport-Measured Γ and K_{IA} values to Directly-Measured Values

The transport-measured Γ data from Figure 4 are combined with the directly-measured data from Figure 2A, and presented in Figure 5. Some of the direct-measured data sets reported in Figure 2A are not included to reduce clutter. Together, data are presented for a total of five PFAS, with three column-measured data sets (PFOA, PFOS, APMO) and three directly-measured data sets (PFOA, PFNA, C6F13PEO). The measured data span approximately 6.5 orders of magnitude in aqueous concentration.

Critically, the transport-measured data are observed to be fully consistent with the directly-measured data. Specifically, Γ values for the two methods are entirely coincident in the region of

overlapping concentrations, which spans \sim 4 orders-of-magnitude. Furthermore, the two data sets adhere to an identical Γ -C profile. The great consistency among Γ data sets measured with different methods by different investigators for different surfactants is quite remarkable. These results conclusively demonstrate the accuracy of the transport-measured values.

The concentration dependency of the column-measured K_{IA} data can be examined now that they have been determined to be robust. K_{IA} values measured from the transport experiments are presented in Figure 6. The K_{IAS} clearly attain constant values at lower concentrations. Furthermore, these constant values are maintained over ~2 orders-of-magnitude. These results clearly demonstrate that transport-measured K_{IAS} are subject to maximum limiting values at lower aqueous concentrations. This is fully consistent with the results obtained for the direct-measurement methods (Figure 3).

4.5 Alternative Analysis of the Concentration Dependency of K_{LA}^{0} and K_{LA}^{0}

The determination of K_{IA} values from transport experiments is generally faced with potential uncertainty due to the need to specify the air-water interfacial area. However, perspicacious use of equations 4 and 5 provides a means to eliminate this uncertainty when examining the condition dependency of K_{IA} . Inspection of equation 5 shows that K_{IA}^0 is a function of K_{IA} , A_{IA} , and θ_w . Notably, the values of A_{IA} and θ_w remain constant for experiments conducted with the same porous medium and water content. Thus, experiments conducted in this manner allow one to investigate the influence of system variables specifically on K_{IA} without the need to specify A_{IA} . For the present study, the concentration dependency of K_{IA}^0 and thus K_{IA} is investigated by examining the results of transport experiments conducted with different input concentrations for the same medium and water content. Even though the K_{IA} values measured from

the transport experiments were demonstrated to be robust in the preceding section, this alternative analysis is conducted to provide an additional, independent means of investigation.

To compare amongst the three PFAS, the K_{IA}^0 values are normalized by dividing by a reference K_{IA}^0 . A standard reference value would be the maximum K_{IA}^0 value for each PFAS. However, it is not desirable to make assumptions about maximum values for this analysis given the focus is on determining the concentration dependency. Hence, an arbitrary reference is selected of K_{IA}^0 (C=1), i.e., the respective value of K_{IA}^0 measured for each PFAS at the input concentration of 1 mg/L. The set of K_{IA}^0 values for each PFAS is scaled by the respective K_{IA}^0 (C=1) for that particular PFAS. Importantly, this normalization procedure preserves the respective profiles of the individual K_{IA}^0 -C functions for each PFAS. The aqueous concentration is not scaled for this analysis.

The normalized K_{IA}^0 values as a function of aqueous concentration are presented in Figure 7. The K_{IA}^0 values asymptotically approach maximum values, which are attained at concentrations of approximately 0.1 to 1 mg/L. There is some variability between the three PFAS, due to non-scaling of the concentrations. PFOS is observed to exhibit a sharper slope than PFOA whereas APMO exhibits a much more moderate slope, both consistent with the respective differences in surface activities. As noted previously, these data represent experiments that were conducted with the same porous medium and similar water contents. Hence, these results demonstrate that K_{IA} values determined from the transport experiments exhibit asymptotic approaches to maximum values for these three PFAS. This conclusion is determined without the need to specify A_{IA} , and therefore is not subject to any uncertainty in that regard. The results of this analysis are consistent with the prior analyses.

4.6 Comparison of Direct, Transport, and ST-Gibbs Measurements

 Γ and K_{IA} values determined by applying the Gibbs adsorption equation to measured surface-tension data for PFOA are presented in Figures 4-6. Inspection of Figure 5 reveals that the ST-Gibbs values are fully consistent with the data obtained by the direct-measurement methods. This illustrates the consistency of ST-Gibbs and direct-measured data discussed in the Theory section. As noted therein, the consistency of the two data sets demonstrates the validity of applying the Gibbs equation to surface/interfacial-tension data to determine Γ and K_{IA} .

Inspection of Figures 4-6 shows that the ST-Gibbs data are consistent with the transport-measured data. This is further examined by comparing the full set of transport-measured K_{IA} values to ST-Gibbs-determined values in Figure 8. Excellent correspondence is exhibited among the large number of measurements (41 total). This data set comprises K_{IA} values determined for solutions of 4 different ionic strengths (1.5, 5, 10, and 30 mM), two ionic compositions (NaCl and CaCl₂), different pHs (5-8), and for tests conducted with different water saturations (ranging from 0.4-0.86) and mean pore-water velocities, and for three PFAS. Hence, the data span a wide range of conditions. These results demonstrate that the Gibbs adsorption equation can be applied to measured surface/interfacial tension data to determine K_{IA} values that are representative for transport conditions.

Specific K_{IA} values determined from NR direct measurements, the transport experiments, and from ST-Gibbs can be compared for further assessment of consistency. This is done for PFOA in 0.01 M NaCl at an aqueous concentration of 10 μ g/L. Any such assessment should account for measurement uncertainty for each of the methods. NR measurements have a reported uncertainty of ~5% (see the relevant references cited for the NR data). The uncertainty associated with the surface-tension measurements and the transport experiments is discussed in section SI-2 of the SI

and section 4.3, respectively. The following K_{IA} values are determined: NR = 0.0032 (0.0030-0.0034), transport = 0.0033 (0.0028-0.0038), and ST-Gibbs = 0.0032 (0.0024-0.0040). The comparison reveals that the mean values for all three are essentially identical. As a result of this consistency, predicted retardation factors calculated using either the NR or ST-Gibbs K_{IA} values match the measured R values obtained from the transport experiments (data not shown). The K_{IA} values as a function of concentration are compared in Figure SI-4. It is observed that the K_{IA} -C profiles for all three measurements are coincident within the measurement uncertainty. The results are consistent with the original comparison reported by Lyu et al. (2018).

Inspection of Figure 5 shows that the Langmuir isotherm provides an excellent match to all of the measured data. It is notable that the isotherm was fit only to the PFOA data obtained from the direct NR measurements. None of the transport-measured data, ST-Gibbs data, or the other directly-measured data were used for the isotherm fitting. This further supports the consistency of the data sets. It also demonstrates that the Langmuir isotherm is appropriate for describing these data over an extremely large (6.5 log) aqueous concentration range and 4-log range in measured interfacial adsorption. The isotherm represents both the linear adsorption observed at lower concentrations, as the Langmuir isotherm reduces to the Henry linear isotherm at low concentrations, while also representing the attainment of maximum interfacial adsorption at high concentrations.

4.7 Surface Coverage and Critical Concentrations

The directly-measured Γ data can be used to characterize relative surface coverage (Γ/Γ_{max}) for fluid-fluid interfacial adsorption. Inspection of Figures 2, 4, and 5 shows that the surface coverages for all 5 PFAS and all 8 hydrocarbon surfactants in different ionic-strength solutions,

and including both air-water and NAPL-water systems, collapse to one master curve upon scaling, as noted above. This illustrates the concurrence of fluid-fluid interfacial adsorption behavior amongst the various systems in terms of relative surface coverage. Hence, surface coverage can be considered a controlling discriminant for surfactant behavior with equivalence and correlation to surface activity.

The normalized K_{IA} is compared to the surface coverage in Figure 9. The concentration at which K_{IA} approaches ~95% of the maximum corresponds to approximately 10% surface coverage. Hence, the region wherein K_{IA} is essentially constant, and for which the measured adsorption isotherm is effectively linear, has surface coverages of <10%. Similar results are obtained using the directly-measured SDS-SDBS data (Figure SI-5).

The expectation of linear fluid-fluid interfacial adsorption at very low surface coverages is widely established in surfactant and surface science (e.g., Chang and Franses, 1995; Eastoe and Dalton, 2000; Berg, 2010; Danov and Kralchevsky, 2012; Romsted, 2014; Tadros, 2015; Lang and Liu, 2016; Aveyard, 2019). This is often referred to as Henry's adsorption. Such ideal, linear behavior is consistent with coverages that are sufficiently low such that lateral interactions amongst adsorbed monomers is minimal and the total occupied area is small relative to the total interfacial area. The linear isotherm and constant K_{IA} observed at low concentrations for the directly-measured data and the transport-measured data are consistent with ideal conditions at low surface coverage.

The specific concentration at which the onset of linear adsorption and constant K_{IA} will be observed for any given surfactant will depend on the surface activity of that particular surfactant and when the degree of surface coverage becomes sufficiently low such that adsorption becomes ideal. In terms of a readily measurable property such as the surface-tension function, Figure SI-6

shows that PFOA surface tension begins to decrease significantly in the range of 10% surface coverage. This is consistent with the results reported for CTAB by Mukherjee et al. (2013). The critical surface coverage for surface-tension reduction is consistent with that for the attainment of K_{IA} constancy.

These results highlight an important point concerning the adsorption behavior of surfactants at fluid-fluid interfaces with regards to concentration-related effects. It is not the actual concentration that is of import, but rather the concentration with respect to the surface activity and degree of surface coverage under the extant conditions. One may define a set of concentration regimes based on correlation of the ranges of PFAS concentrations observed in environmental systems of interest to transport phenomenon of import. For the example of PFAS adsorption at fluid-fluid interfaces, the critical concentrations at which K_{IA} values approach their maximum are likely to be higher than measured concentrations at many (but not all) sites, as noted by Brusseau (2019a). The critical concentrations may be lower than measured concentrations for example at some AFFF source zones. This approach can be applied to other transport phenomena of relevance to PFAS fate in the environment.

5. Conclusions

Direct, high-resolution measurements of surfactant adsorption at the air-water and NAPL-water interface were aggregated from the literature. These data represent the most accurate and robust measurements of Γ and K_{IA} values that exist to date. This data set provides a gold-standard benchmark for evaluating the accuracy of measurements based on transport experiments, surface-tension measurements, and other methods. It is anticipated that this data set will be useful for future

development and testing of methods for measurement and estimation of PFAS adsorption at fluidfluid interfaces.

The largest data set to date of Γ and K_{IA} values measured from transport experiments was compiled from several miscible-displacement studies investigating the transport of PFAS in unsaturated porous media. Although the need to specify A_{IA} can be an impediment to accurate determination of K_{IA} values from transport experiments, the use of highly characterized media with robust measures of A_{IA} minimized this issue for the present study. Γ and K_{IA} values determined from the transport-measured data were observed to be fully consistent with the directly-measured data. These results conclusively demonstrate the accuracy of the transport-measured values. This in turn validates the efficacy of the methods used for the transport experiments and the values used for A_{IA} . Γ and K_{IA} values determined from the application of the Gibbs equation to measured surface-tension data were fully consistent with the directly-measured and transport-measured data.

The directly-measured data were used to examine the concentration dependency of K_{IA} values, which clearly demonstrated that K_{IA} attains a constant, maximum value at lower concentrations. Two separate analyses of the transport-measured data both produced observations of constant K_{IA} values at lower concentrations, consistent with the directly-measured data. The critical concentration at which adsorption is effectively linear and K_{IA} approaches its maximum depends on the relative surface coverage, which is a function of the surface activity of the particular PFAS under the extant conditions. The importance of evaluating concentrations in terms of surface activities and surface coverage, and the concept of defining critical concentrations in reference to PFAS transport phenomena of interest was discussed.

The outcomes of this study should be of relevance to the characterization and modeling of PFAS transport and fate in multiple environmental systems. The results of this study elucidate the fundamental concentration-dependency behavior for PFAS fluid-fluid interfacial adsorption. However, the actual magnitudes and significance of interfacial adsorption, particularly for field systems, are a function of a number of factors and other processes as described in prior studies (e.g., Brusseau, 2018, 2019b, 2020; Brusseau and Van Glubt, 2019; Brusseau et al., 2019a, 2019b; Guo et al., 2020). The impacts of factors such as soil physical and geochemical heterogeneity and PFAS mixtures require further investigation.

Acknowledgements

This research was supported by the NIEHS Superfund Research Program (P42 ES04940) and by the National Science Foundation (2023351). Sarah Van Glubt is thanked for her assistance with the surface-tension measurements. The reviewers are thanked for their constructive comments.

Figure Captions

Figure 1. Adsorption of surfactant C8Tempo at the air-water interface measured directly with horizontal-touch voltammetry (HTV) and Brewster angle microscopy (BAM), and determined from application of the Gibbs adsorption equation to measured surface-tension data (ST-Gibbs). The solid line represents the best-fit Langmuir isotherm to the aggregated data. Data reproduced from Malec et al. (2004).

Figure 2. Direct measurements of surfactant adsorption (Γ) at the air-water and NAPL-water interface. (A) All data, with scaled aqueous concentrations; (B) non-scaled data for sodium dodecyl sulfate (SDS) and sodium decylbenzene sulfonate (SDBS) combined (air-water only). Data compiled from the literature (see Table SI-1). The aqueous concentrations are scaled to match the surface activity of PFOA. The scaling factors (S_f) and Γ_{max} values are presented in Table SI-1. BAM = Brewster angle microscopy, Bubble = bubble generation, emulsion = emulsion formation, HTV = horizontal touch voltammetry, IRRAS = infrared reflection absorption spectroscopy, NICISS = neutral impact collision ion scattering spectroscopy, NR = neutron reflectometry, RT= radiotracer, Surf Pot = surface potential, VSFS = vibrational sum frequency spectroscopy; O-W represents a NAPL-water system.

Figure 3. Fluid-fluid interfacial adsorption coefficients (K_{IA}) determined from the directly measured data reported in Figure 2. (A) Entire data set reported in Figure 2A; (B) non-scaled data for sodium dodecyl sulfate (SDS) and sodium decylbenzene sulfonate (SDBS) from Figure 2B (air-water only).

Figure 4. Measured air-water and NAPL-water (O-W) interfacial adsorption from transport experiments and from application of the Gibbs adsorption equation to measured PFOA surface-tension data (ST-Gibbs).

Figure 5. Comparison of measured fluid-fluid interfacial adsorption determined from transport experiments (closed symbols) reported in Figure 5 and from direct-measurement methods (open symbols) reported in Figure 2A. Values are also reported from application of the Gibbs adsorption equation to measured PFOA surface-tension data (ST-Gibbs). The Langmuir isotherm was fit to only the PFOA data measured directly with neutron reflectivity; no other data were used for the optimization.

Figure 6. Concentration dependency of K_{IA} values measured from transport experiments. Values are also reported from application of the Gibbs adsorption equation to measured PFOA surfacetension data (ST-Gibbs).

Figure 7. Analysis of concentration dependency of K_{IA}^0 . Note that three and two measurements are represented by the PFOA and PFOS data points, respectively, at C = 1. The line is shown for visualization purposes.

Figure 8. One-to-one comparison of K_{IA} values measured from transport experiments and application of the Gibbs equation to measured surface-tension data.

Figure 9. Normalized K_{IA} versus surface coverage (Γ/Γ_{max}) determined from directly-measured data reported in Figures 2A and 3A, respectively.

References

Ahrens, L., 2011. Polyfluoroalkyl compounds in the aquatic environment: a review of their occurrence and fate. J. Environ. Monit. 13, 20-31.

Ahrens, L., Shoeib, M., Harner, T., Lee, S.C., Guo, R., Reiner, E.J., 2011. Wastewater treatment plant and landfills as sources of polyfluoroalkyl compounds to the atmosphere. Environ. Sci. Technol., 45, 8098–8105.

An, S.W., Lu, J.R., Thomas, R.K., and Penfold, J., 1996. Apparent anomalies in surface excesses determined from neutron reflection and the Gibbs equation in anionic surfactants with particular reference to perfluorooctanoates at the air/water interface. Langmuir 12(10), 2446-2453.

Anderson, R.H., Adamson, D.T., and Stroo, H.F., 2019. Partitioning of poly-and perfluoroalkyl substances from soil to groundwater within aqueous film-forming foam source zones. J. Contam. Hydrol. 220, 59-65.

Anwar, A., Bettahar, M., Matsubayashi, U.J., 2000. A method for determining air—water interfacial area in variably saturated porous media. J. Contam. Hydrol. 43, 129–146.

Araujo, J.B., Brusseau, M.L., 2019. Novel fluid-fluid interface domains in geologic media. Environ. Sci.: Proc. Impacts, 21, 145–154.

Araujo, J.B., Brusseau, M.L., 2020. Assessing XMT-measurement variability of air-water interfacial areas in natural porous media. Water Resour. Res., 56, e2019WR025470.

Araujo, J.B., Mainhagu, J., Brusseau, M.L., 2015. Measuring air-water interfacial area for soils using the mass balance surfactant-tracer method. Chemo., 134, 199-202.

Aveyard, B., 2019. **Surfactants: In Solution, at Interfaces and in Colloidal Dispersions**. Oxford University Press, Oxford.

Berg, J.C., 2010. An Introduction to Interfaces & Colloids: the Bridge to Nanoscience. World Scientific Publishing Co, Singapore.

Brusseau, M.L., 2018. Assessing the potential contributions of additional retention processes to PFAS retardation in the subsurface. Sci. Total Environ. 613-614, 176-185.

Brusseau, M.L., 2019a. The influence of molecular structure on the adsorption of PFAS to fluid-fluid interfaces: using QSPR to predict interfacial adsorption coefficients. Water Res. 152, 148-158.

Brusseau, M.L., 2019b. Estimating the relative magnitudes of adsorption to solid-water and air/oil-water interfaces for per-and poly-fluoroalkyl substances. Environ. Poll., 254, article 113102.

Brusseau, M.L., 2020. Simulating PFAS transport influenced by rate-limited multi-process retention. Water Res., 168, article 115179.

Brusseau, M.L. and Van Glubt, S., 2019. The influence of surfactant and solution composition on PFAS adsorption at fluid-fluid interfaces. Water Res. 161, 17–26.

Brusseau, M.L., Peng, S., Schaar, G., Costanza-Robinson, M.S., 2006. Relationships among airwater interfacial area, capillary pressure, and water saturation for a sandy porous medium. Water Resour. Res. 42, W03501

Brusseau, M.L., Peng, S., Schnaar, G., and Murao, A. 2007. Measuring air-water interfacial areas with x-ray microtomography and interfacial partitioning tracer tests. Environ. Sci. Technol., 41, 1956-1961.

Brusseau, M.L., Janousek, H., Murao, A., and Schnaar, G. 2008. Synchrotron x-ray microtomography and interfacial partitioning tracer test measurements of NAPL-water interfacial areas. Water Resour. Res., Vol. 44, W01411, doi:10.1029/2006WR005517.

Brusseau, M.L., Yan, N., Van Glubt, S., Wang, Y., Chen, W., Lyu, Y., Dungan, B., Carroll, K.C., Holguin, F.O., 2019a. Comprehensive retention model for PFAS transport in subsurface systems. Water Res. 148, 41-50.

Brusseau, M.L., Khan, N., Wang, Y., Yan, N., Van Glubt, S., Carroll, K.C., 2019b. Nonideal transport and extended elution tailing of PFOS in soil. Environ. Sci. Technol. 53, 10654-10664.

Brusseau, M.L., Anderson, R.H., Guo, B., 2020. PFAS concentrations in soils: Background levels versus contaminated sites. Sci. Total Environ. 740, 140017.

Chang, C-H. and Franses, E.I., 1995. Adsorption dynamics of surfactants at the air/water interface: A critical review of mathematical models, data, and mechanisms. Coll. Surf. A., 100, 1-45.

Chattoraj, D.K. and Birdi, K.S. **Adsorption and the Gibbs Surface Excess**. 1984. Plenum Press, New York, NY.

Cousins, I.T., Vestergren, R., Wang, Z., Scheringer, M., McLachlan, M.S., 2016. The precautionary principle and chemicals management: the example of perfluoroalkyl acids in groundwater. Environ. Int. 94, 331-340.

Dai, X.D., Xie, Z.L., Dorian, B., Gray, S., Zhang, J.H., 2019. Comparative study of PFAS treatment by UV, UV/ozone, and fractionations with air and ozonated air. Environ. Sci.: Water Res. Technol., 5,1897-1907.

Danov, K.D. and Kralchevsky, P.A., 2012. The standard free energy of surfactant adsorption at air/water and oil/water interfaces: Theoretical vs. empirical approaches. Colloid J., 74, 172–185.

Dauchy, X., Boiteux, V., Colin, A., Hemard, J., Bach, C., Rosin, C., Munoz, J.-F., 2019. Deep seepage of per-and polyfluoroalkyl substances through the soil of a firefighter training site and subsequent groundwater contamination. Chemo 214, 729–737.

Davies, J.T. and Rideal, E.K., 1961. Interfacial Phenomenon. Academic Press, New York, NY.

Defay, R., Prigogine, I., and Bellemans, A., 1966. **Surface Tension and Adsorption**. John WIley & Sons, Hew York, NY.

Downer, A., Eastoe, J., Pitt, A.R., Penfold, J., Heenan, R.K., 1999a. Adsorption and micellisation of partially- and fully-fluorinated surfactants. Colloids Surfs. A, 156, 33-48.

Downer, A., Eastoe, J., Pitt, A.R., Simister, E.A., Penfold, J., 1999b. Effects of hydrophobic chain structure on adsorption of fluorocarbon surfactants with either CF3– or H–CF2– terminal groups. Langmuir 15, 7591-7599.

Downes, N., Ottewill, G.A., Ottewill, R.H., 1995. An investigation of the behaviour of ammonium perfluoro-octanoate at the air/water interface in the absence and presence of salts. Colloids Surfs. A, 102, 203-211.

Dupont, A., Eastoe, J., Barthélémy, P., Pucci, B., Heenan, R., Penfold, J., Steytler, D.C., and Grillo, I., 2003. Neutron reflection and small-angle neutron scattering studies of a fluorocarbon telomer surfactant. J. Coll. Inter. Sci., 261, 184-190.

Eastoe, J. and Dalton, J.S., 2000. Dynamic surface tension and adsorption mechanisms of surfactants at the air-water interface. Adv. Colloid Interface Sci., 85, 103-144.

Eastoe, J., Nave, S., Downer, A., Paul, A., Rankin, A., Tribe, K., Penfold, J., 2000. Adsorption of ionic surfactants at the air—solution interface. Langmuir 16, 4511-4518.

Eastoe, J., Paul, A., Rankin, A., Wat, R., Penfold, J., Webster, J.R., 2001. Fluorinated nonionic surfactants bearing either CF3– or H– CF2– terminal groups: Adsorption at the surface of aqueous solutions. Langmuir 17, 7873-7878.

Eastoe, J., Rankin, A., Wat, R., Bain, C.D., Styrkasm D., and Penfold, J., 2003. Dynamic surface excesses of fluorocarbon surfactants. Langmuir, 19, 7734-7739.

Eastoe, J., Rogers, S.E., Martin, L.J., Paul, A., Guittard, F., Guittard, E., Heenan, R.K., Webster, J.R., 2006. Fluorosurfactants at structural extremes: Adsorption and aggregation. Langmuir 22, 2034-2038.

El Ouni, A., Guo, B., Zhong, H., and Brusseau, M.L. 2021. Testing the validity of the miscible-displacement interfacial tracer method for measuring air-water interfacial area: Independent benchmarking and mathematical modeling. Chemo., 263, article 128193.

Fainerman, V.B., Miller, R., and Mohwald, H., 2002. General relationships of the adsorption behavior of surfactants at the water/air interface. J. Phys. Chem. B, 106, 809-819.

Guo, B., Zeng, J., and Brusseau, M.L. 2020. A mathematical model for the release, transport, and retention of per-and polyfluoroalkyl substances (PFAS) in the vadose zone. Water Resources Research, 56 (2), e2019WR026667.

Gurkov, T.D., Dimitrova, D.T., Marinova, K.G., Bilke-Crause, C., Gerber, C., and Ivanov, I.B., 2005. Ionic surfactants on fluid interfaces: determination of the adsorption; role of the salt and the type of the hydrophobic phase. Colloids Surf. A Physicochem. Eng. Asp. 261, 29–38.

Hatton, J., Holton, C., and DiGuiseppi, B., 2018. Occurrence and behavior of per- and polyfluoroalkyl substances from aqueous film-forming foam in groundwater systems. Remediation 28, 89-99.

Hill, C., Czajka, A., Hazell, G., Grillo, I., Rogers, S.E., Skoda, M.W.A., Joslin, N., Payne, J., Eastoe, J., 2018. Surface and bulk properties of surfactants used in fire-fighting. J. Colloid Interface Sci. 530, 686-694.

Hines, J.D., Thomas, R.K., Garrett, P.R., Rennie, G.K., Penfold, J., 1997. Investigation of mixing in binary surfactant solutions by surface tension and neutron reflection: anionic/nonionic and zwitterionic/nonionic mixtures. J. Phy. Chem. B, 101, 9215-9223.

Høisæter, Å., Pfaff, A., and Breedveld, G.D., 2019. Leaching and transport of PFAS from aqueous film-forming foam (AFFF) in the unsaturated soil at a firefighting training facility under cold climatic conditions. J. Contam. Hydrol., 222, 112–122.

Jiang, H., Guo, B., and Brusseau, M.L., 2020. Pore-scale modeling of fluid-fluid interfacial area in variably saturated porous media containing micro-scale surface roughness. Water Resour. Res. 56 article: e2019WR025876.

Kim, H., Rao, P.S.C., and Annable, M.D. 1997. Determination of effective air—water interfacial area in partially saturated porous media using surfactant adsorption. Water Resour. Res. 33 (12), 2705–2711.

Lang, P.R. and Liu, Y., 2016. **Soft Matter at Aqueous Interfaces**. Springer International Publishing, Switzerland.

Li, Z., Lyu, X., Gao, B., Xu, H., Wu, J., Sun, Y., 2021. Effects of ionic strength and cation type on the transport of perfluorooctanoic acid (PFOA) in unsaturated sand porous media. J. Hazard. Mat., 403, 123688.

Lu, J.R., Lee, E.M., Thomas, R.K., Penfold, J., Flitsch, S.L., 1993. Direct determination by neutron reflection of the structure of triethylene glycol monododecyl ether layers at the air/water interface. Langmuir 9, 1352-1360.

Lunkenheimer, K., Prescher, D., Hirte, R., Geggel, K. 2015. Adsorption properties of surface chemically pure sodium perfluoro-n-alkanoates at the air/water interface: counterion effects within homologous series of 1:1 ionic surfactants. Langmuir 31, 970-981.

Lyu, Y. and Brusseau, M.L., 2020. The influence of solution chemistry on air-water interfacial adsorption and transport of PFOA in unsaturated porous media. Sci. Total Environ., 713, 136744.

Lyu, Y., Brusseau, M.L., Ouni, A.E., Araujo, J.B., and Su, X., 2017. The gas-absorption/chemical-reaction method for measuring air-water interfacial area in natural porous media. Water Resour. Res. 53, 9519-9527.

Lyu, Y., Brusseau, M.L., Chen, W., Yan, N., Fu, X., Lin, X., 2018. Adsorption of PFOA at the airwater interface during transport in unsaturated porous media. Environ. Sci. Technol. 52, 7745-7753.

Lyu, X., Liu, X., Sun, Y., Gao, B., Ji, R., Wu, J., and Xue, Y., 2020. Importance of surface roughness on perfluorooctanoic acid (PFOA) transport in unsaturated porous media. Environ. Poll., 266, article 115343.

Malec, A.D., Wu, D.G., Louie, M., Skolimowski, J.J., Majda, M., 2004. Gibbs monolayers at the air/water interface: Surface partitioning and lateral mobility of an electrochemically active surfactant. Langmuir 20, 1305-1310.

Martínez-Balbuena, L., Arteaga-Jiménez, A., Hernández-Zapata, E., Márquez-Beltrán, C., 2017. Applicability of the Gibbs Adsorption Isotherm to the analysis of experimental surface-tension data for ionic and nonionic surfactants. Adv. Coll. Inter. Sci., 247, 178-184.

Matuura, R., Kimizuka, H., Matsubara, A., Matsunobu, K., and Matsuda, T., 1962. Study of the adsorption of detergents at a solution-air interface by the radiotracer method. V. The effect of inorganic salts on the surface behavior of the dodecyl sulfate ion. Bull. Chem. Society Japan, 35, 552-555.

McGuire, M.E.; Schaefer, C.; Richards, T.; Backe, W. J.; Field, J. A.; Houtz, E.; Sedlak, D.L.; Guelfo, J.L.; Wunsch, A.; Higgins, C.P. 2014, Evidence of remediation-induced alteration of

subsurface poly- and perfluoroalkyl substance distribution at a former firefighter training area. Environ. Sci. Technol. 48 (12), 6644–6652.

McKenzie, E.R., Siegrist, R.L., McCray, J.E., Higgins, C.P. 2016. The influence of a non-aqueous phase liquid (NAPL) and chemical oxidant application on perfluoroalkyl acid (PFAA) fate and transport. Water Res. 92: 199-207.

McMurdo, C.J., Ellis, D.A., Webster, E., Butler, J., Christensen, R.D., Reid, L.K., 2008. Aerosol enrichment of the surfactant PFO and mediation of the water—air transport of gaseous PFOA. Environ. Sci. Technol., 42, 3969-3974.

Meng, P., S.B. Deng, S. Deng, , X. Lu, Z. Du, B. Wang, J. Huang, Y. Wang, G. Yu, B. Xing. 2014. Role of air bubbles overlooked in the adsorption of perfluorooctanesulfonate on hydrophobic carbonaceous adsorbents. Environ. Sci. Technol., 48, 13785–13792

Miyajima, K., Yoshida, H., Maetani, J., and Nakagaki, M., 1980. Studies on the aqueous solutions of guanidinium bromide on the surface tension of aqueous solutions of the cationic surfactants. Bull. Chem. Society Japan, 53, 1523-1529.

Moody, C.A.; Hebert, G.N.; Strauss, S.H.; Field, J.A., 2003. Occurrence and persistence of perfluorooctanesulfonate and other perfluorinated surfactants in groundwater at a fire-training area at Wurtsmith air force base, Michigan, USA. J. Environ. Monit. 5: 341–345.

Mukherjee, I., Moulik, S.P., Rakshit, A.K., 2013. Tensiometric determination of Gibbs surface excess and micelle point: A critical revisit. J. Coll. Inter. Sci., 394, 329-336.

Muramatsu, M., Tajima, L., Iwahashi, M.m Nukina, K., 1973. Adsorption of tritiated surfactants at nitrogen/solution interfaces, as determined by sheet scintillation counting. J. Coll. Inter. Sci., 43, 499-510.

Nave, S., Eastoe, J., and Penfold, J., 2000. What is so special about Aerosol-OT? 1. Aqueous systems. Langmuir 2000, 16, 8733-8740.

Prevedouros, K., Cousins, I.T., Buck, R.C., Korzeniowski, S.H. 2006., Sources, fate, and transport of perfluorocarboxylates. Environ. Sci. Technol., 40, 32–44.

Psillakis, E., Cheng, J., Hoffmann, M.R., Colussi, A.J., 2009. Enrichment factors of perfluoroalkyl oxoanions at the air/water interface. J. Physical Chem. A Lett., 113: 8826-8829.

Radke, C.J., 2015. Gibbs adsorption equation for planar fluid–fluid interfaces: Invariant formalism. Adv. Coll. Inter. Sci., 222, 600-614.

Rauert, C., Shoeib, M. Schuster, J.K., Eng, A., and Harner T., 2018. Atmospheric concentrations and trends of poly- and perfluoroalkyl substances (PFAS) and volatile methyl siloxanes (VMS) over 7 years of sampling in the Global Atmospheric Passive Sampling (GAPS) Network. Environ Pollut., 238:94-102.

Reth, M.; Berger, U., Broman, D., Cousins, I.T., Nilsson, E.D., McLachlan, M.S., 2011. Water-to-air transfer of perfluorinated carboxylates and sulfonates in a sea spray simulator. Environ. Chem., 8, 381–388.

Richards, R.W., Sarica, J., Webster, J.R.P., Holt, S.A., 2003. Direct determination by neutron reflectometry of the distribution of hydrophobically end capped polyethylene oxide at the air/water interface. Langmuir, 19, 7768-7777.

Romsted, L.S., 2014. Surfactant Science and Technology. CRC Press, Boca Raton, FL.

Rontu, N., and Vaida, V., 2007. Surface partitioning and stability of pure and mixed films of 8-2 fluorotelomer alcohol at the air-water interface. J. Phys. Chem. C, 111, 11612-11618.

Schaefer, C.E., DiCarlo, D.A., Blunt, M.J., 2000. Experimental measurement of air-water interfacial area during gravity drainage and secondary imbibition in porous media. Water Resour. Res. 36, 885-890.

Sekine, M., Campbell, R.A., Valkovska, D.S., Day, J.P., Curwen, T.D., Martin, L.J., Holt, S.A., Eastoe, J., Bain, C.D., 2004. Adsorption kinetics of ammonium perfluorononanoate at the air—water interface. Phys. Chem. Chem. Phy., 6, 5061-5065.

Simcik, M. F. 2005. Global transport and fate of perfluorochemicals. J. Environ. Moni. 7, 759-76.

Simister, E.A., Lee, E.M., Lu, J.R., Ottewill, R.H., Rennie, A.R., Penfold, J., 1992. Adsorption of ammonium perfluorooctanoate and ammonium decanoate at the air/solution interface. J. Chem. Soc. Faraday Trans., 88, 3033-3041.

Snavely, E.S., Schmid, G.M., and Hurd, R.M., 1962. Simple experimental method for verification of the Gibbs adsorption equation. Nature, 194, 439-441.

Tadros, T.F., 2015. Interfacial Phenomena and Colloid Stability. Walter de Gruyter GmbH, Berlin.

Tajima, L., Muramatsu, M., and Sasaki, T., 1970. Radiotracer studies on adsorption of surface active substance at aqueous surface. I. Accurate measurement of adsorption of tritiated sodium, dodecylsulfate. Bull. Chem. Soc. Japan., 43, 1991-1998.

Van Glubt, S., Brusseau, M.L., Yan, N., Huang, D., Khan, N., and Carroll, K.C., 2001. Column versus batch methods for measuring PFAS adsorption to geomedia. Environ. Poll., 268, article 115917

Vecitis, C.D., Park, H., Cheng, J., Mader, B.T., Hoffmann, M.R., 2008. Enhancement of perfluorooctanoate (PFOA) and perfluorooctanesulfonate (PFOS) activity at acoustic cavitation bubble interfaces. J. Phys. Chem. 112, 16850-16857.

Weber, A.K., Barber, L.B., LeBlanc, D.R., Sunderland, E.M., and Vecitis, C.D., 2017. Geochemical and hydrologic factors controlling subsurface transport of poly- and perfluoroalkyl substances, Cape Cod, Massachusetts. Environ. Sci. Technol., 51, 4269–4279.

Xiao, F., 2017. Emerging poly- and perfluoroalkyl substances in the aquatic environment: a review of current literature. Water Res. 124, 482e495.

Xiao, F., Simcik, M.F., Halbach, T.R., and Gulliver, J.S., 2015. Perfluorooctane sulfonate (PFOS) and perfluorooctanoate (PFOA) in soils and groundwater of a US Metropolitan area: Migration and implications for human exposure. Water Res., 72, 64–74.

Yan, N., Ji, Y., Zhang, B., Zheng, X., and Brusseau, M.L., 2000. Transport of GenX in saturated and unsaturated porous media. Environ. Sci. Technol., 54, 11876-11885.

Zhong, H., El Ouni, A., Lin, D., Wang, B., and Brusseau, M.L. 2016. The two-phase flow IPTT method for measurement of nonwetting-wetting liquid interfacial areas at higher nonwetting saturations in natural porous media, Water Resour. Res., 52, 5506–5515.

FIGURES

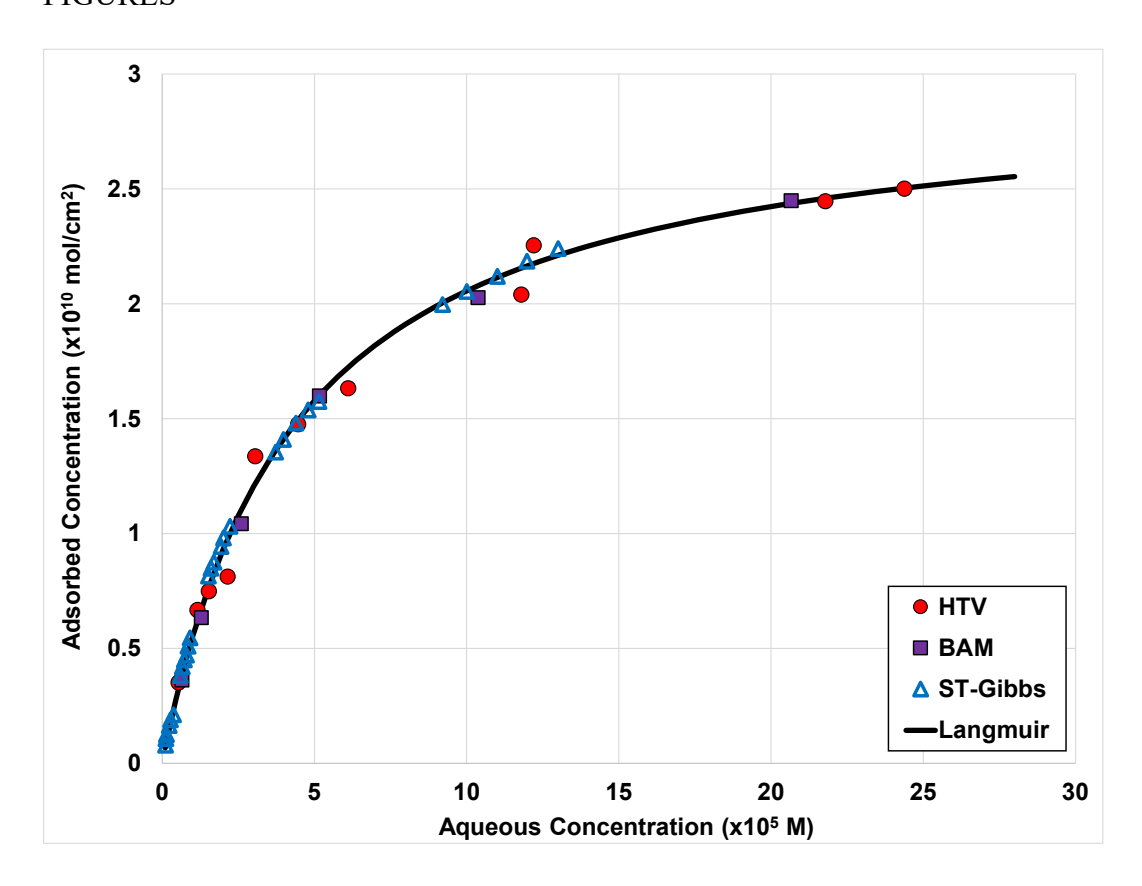
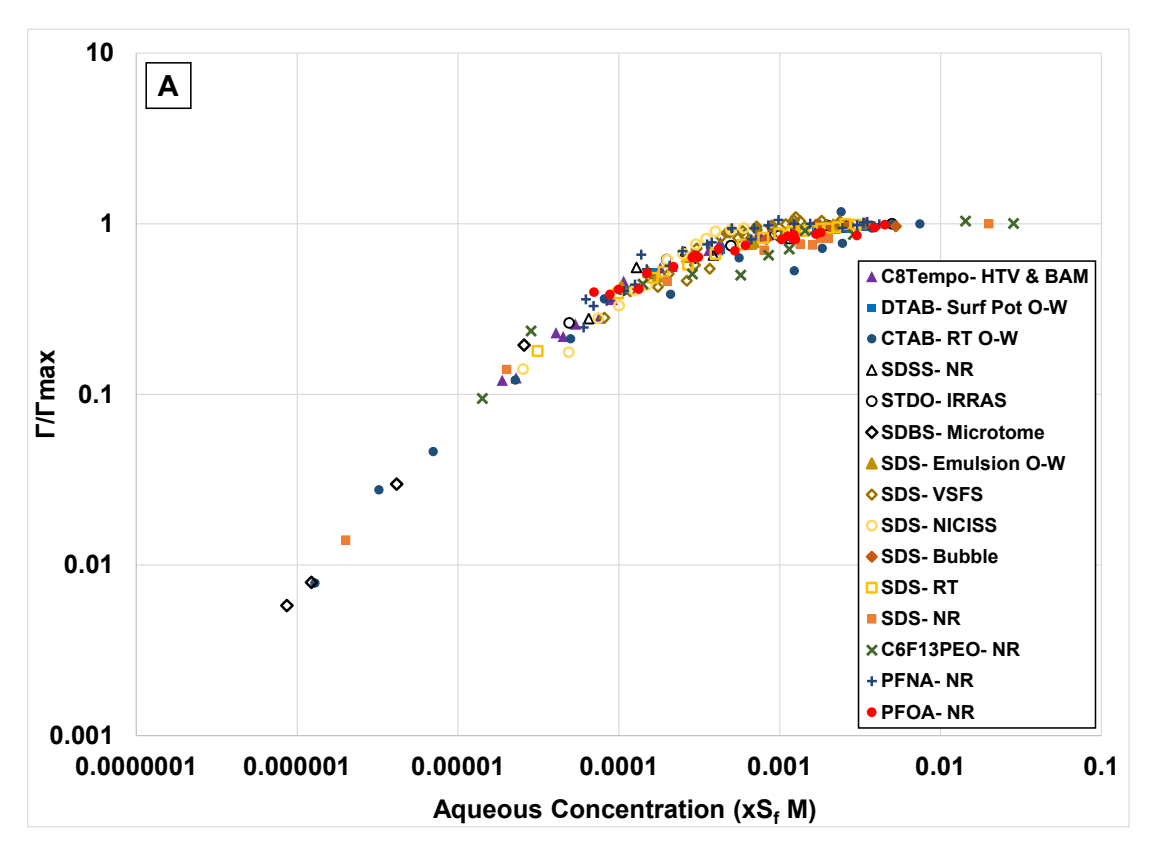


Figure 1. Adsorption of surfactant C8Tempo at the air-water interface measured directly with horizontal-touch voltammetry (HTV) and Brewster angle microscopy (BAM), and determined from application of the Gibbs adsorption equation to measured surface-tension data (ST-Gibbs). The solid line represents the best-fit Langmuir isotherm to the aggregated data. Data reproduced from Malec et al. (2004).



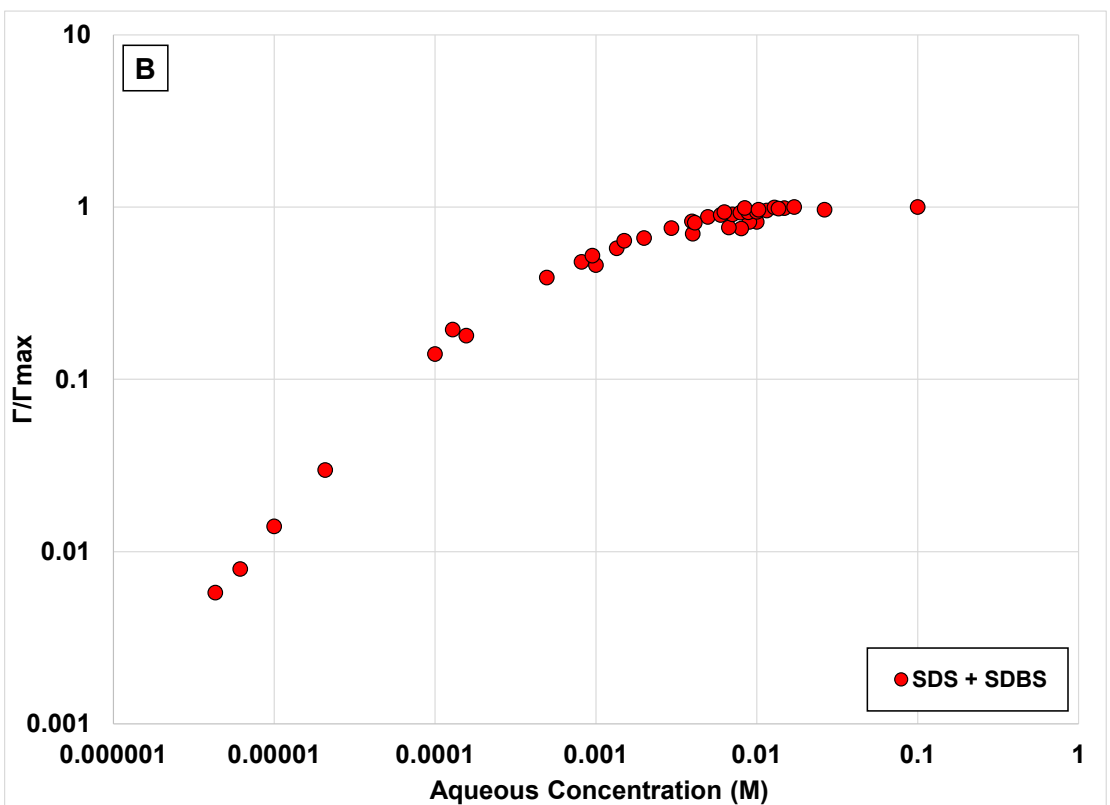
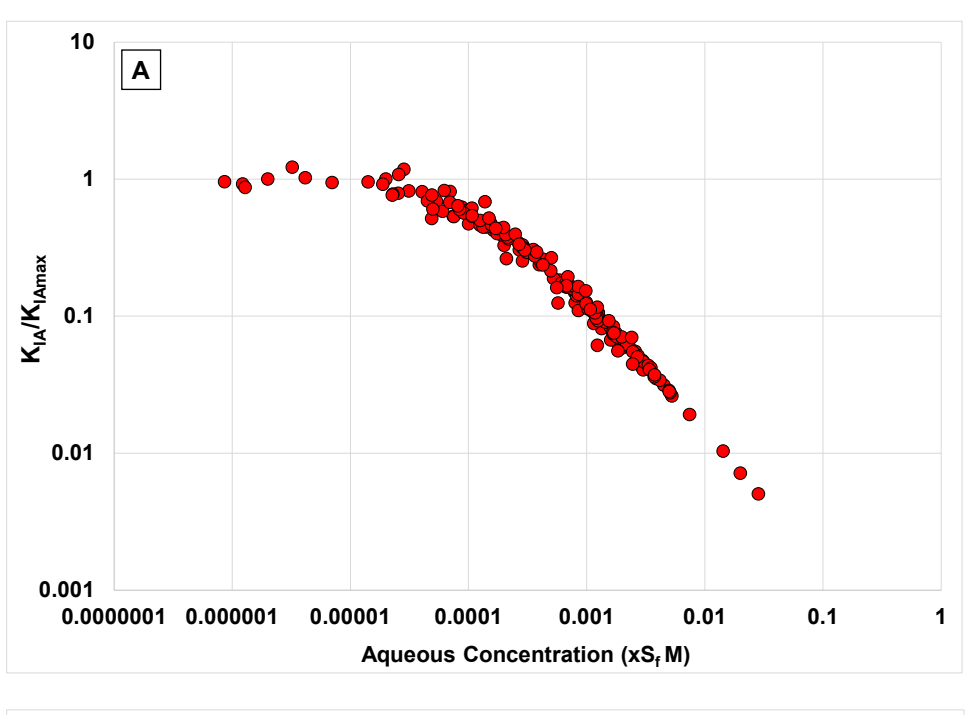


Figure 2. Direct measurements of surfactant adsorption (Γ) at the air-water and NAPL-water interface. (A) All data, with scaled aqueous concentrations; (B) non-scaled data for sodium dodecyl sulfate (SDS) and sodium decylbenzene sulfonate (SDBS) combined (air-water only). Data compiled from the literature (see Table SI-1). The aqueous concentrations are scaled to match the surface activity of PFOA. The scaling factors (S_f) and Γ_{max} values are presented in Table SI-1. BAM = Brewster angle microscopy, Bubble = bubble generation, emulsion = emulsion formation, HTV = horizontal touch voltammetry, IRRAS = infrared reflection absorption spectroscopy, NICISS = neutral impact collision ion scattering spectroscopy, NR = neutron reflectometry, RT= radiotracer, Surf Pot = surface potential, VSFS = vibrational sum frequency spectroscopy; O-W represents a NAPL-water system.



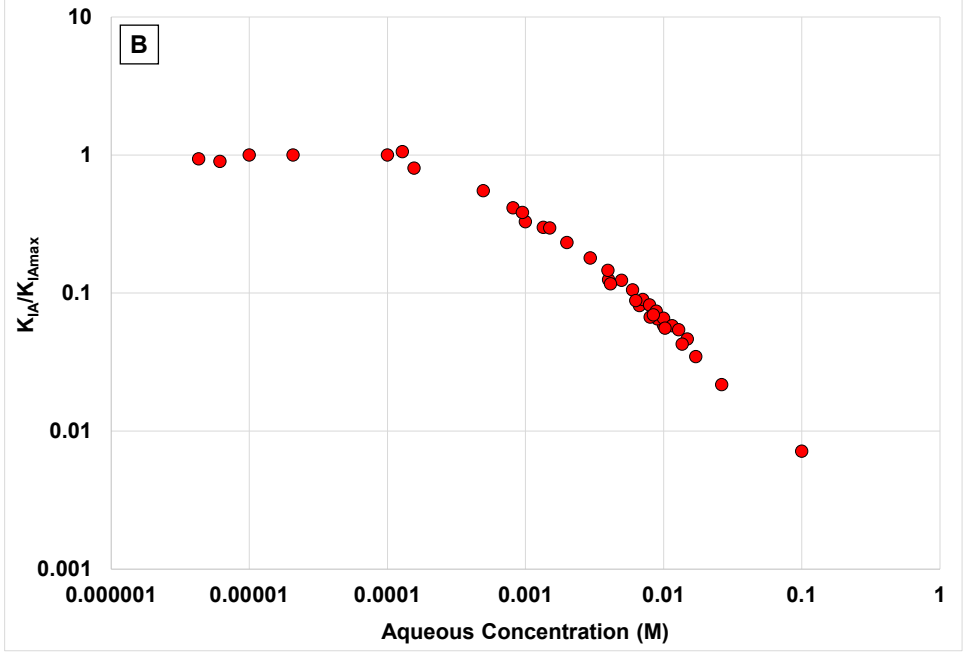


Figure 3. Fluid-fluid interfacial adsorption coefficients (K_{IA}) determined from the directly measured data reported in Figure 2. (A) Entire data set reported in Figure 2A; (B) non-scaled data for sodium dodecyl sulfate (SDS) and sodium decylbenzene sulfonate (SDBS) from Figure 2B (air-water only).

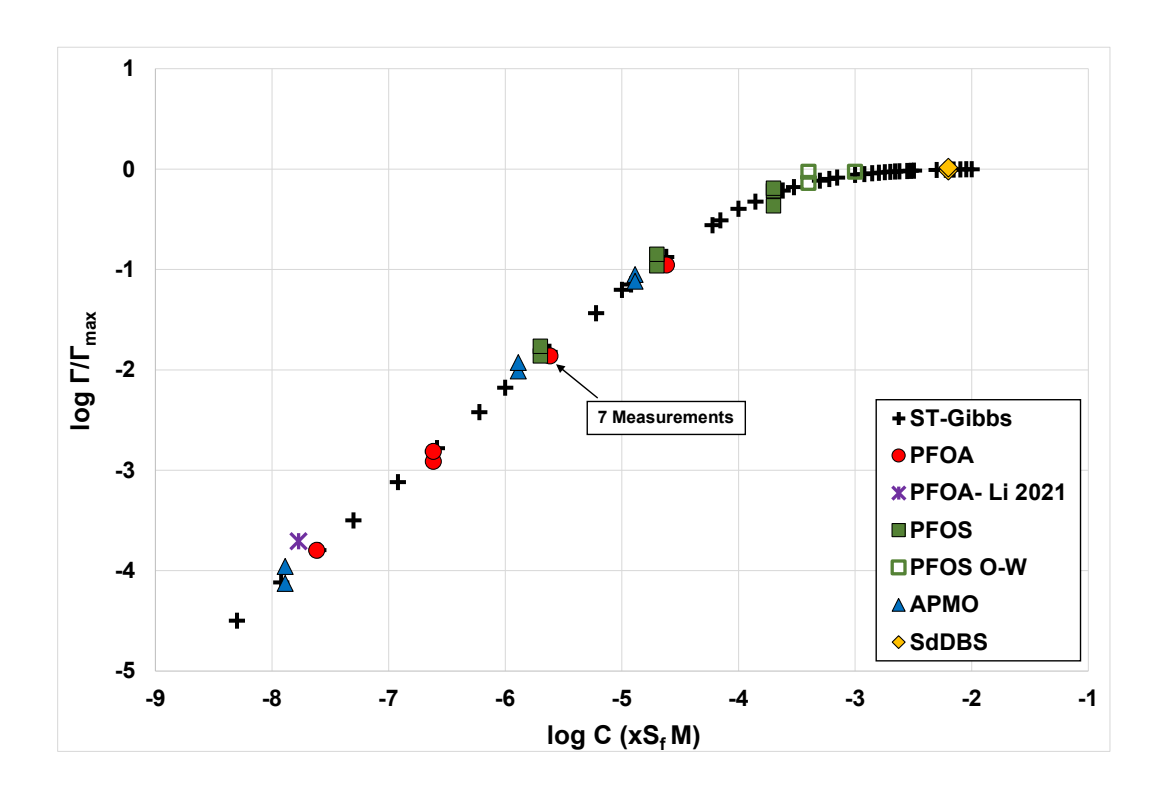


Figure 4. Measured air-water and NAPL-water (O-W) interfacial adsorption from transport experiments and from application of the Gibbs adsorption equation to measured PFOA surface-tension data (ST-Gibbs).

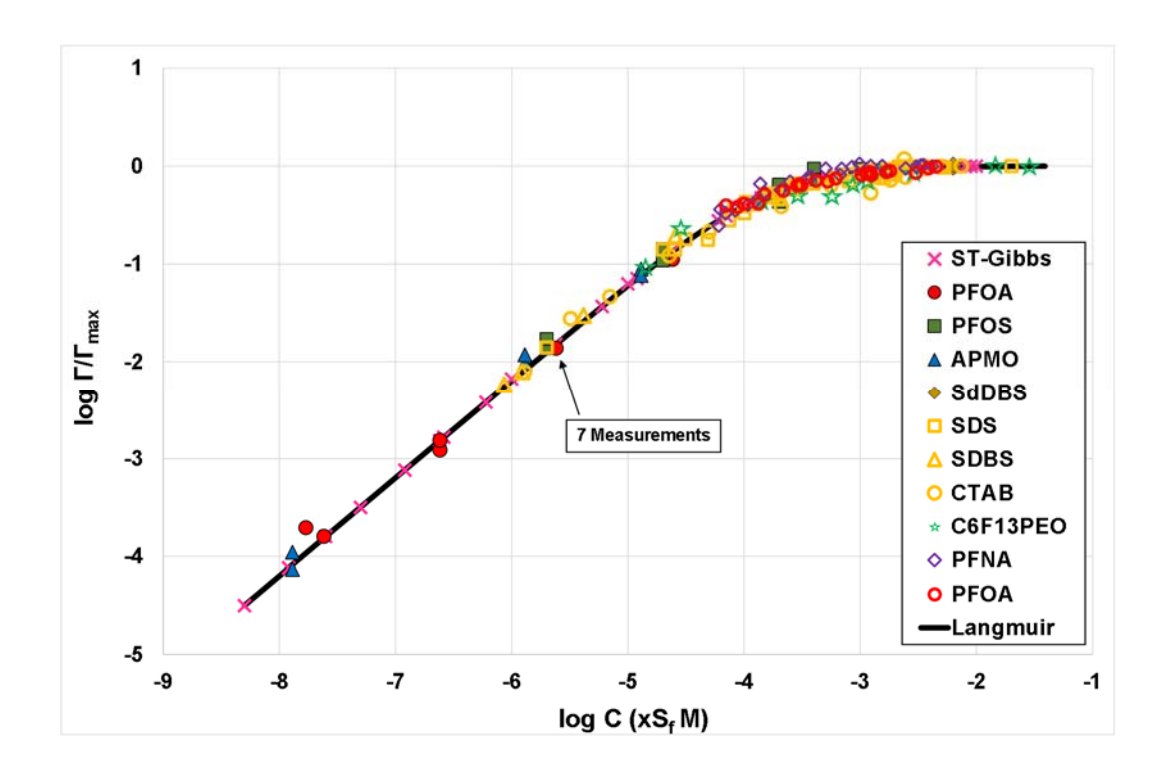


Figure 5. Comparison of measured fluid-fluid interfacial adsorption determined from transport experiments (closed symbols) reported in Figure 5 and from direct-measurement methods (open symbols) reported in Figure 2A. Values are also reported from application of the Gibbs adsorption equation to measured PFOA surface-tension data (ST-Gibbs). The Langmuir isotherm was fit to only the PFOA data measured directly with neutron reflectivity; no other data were used for the optimization.

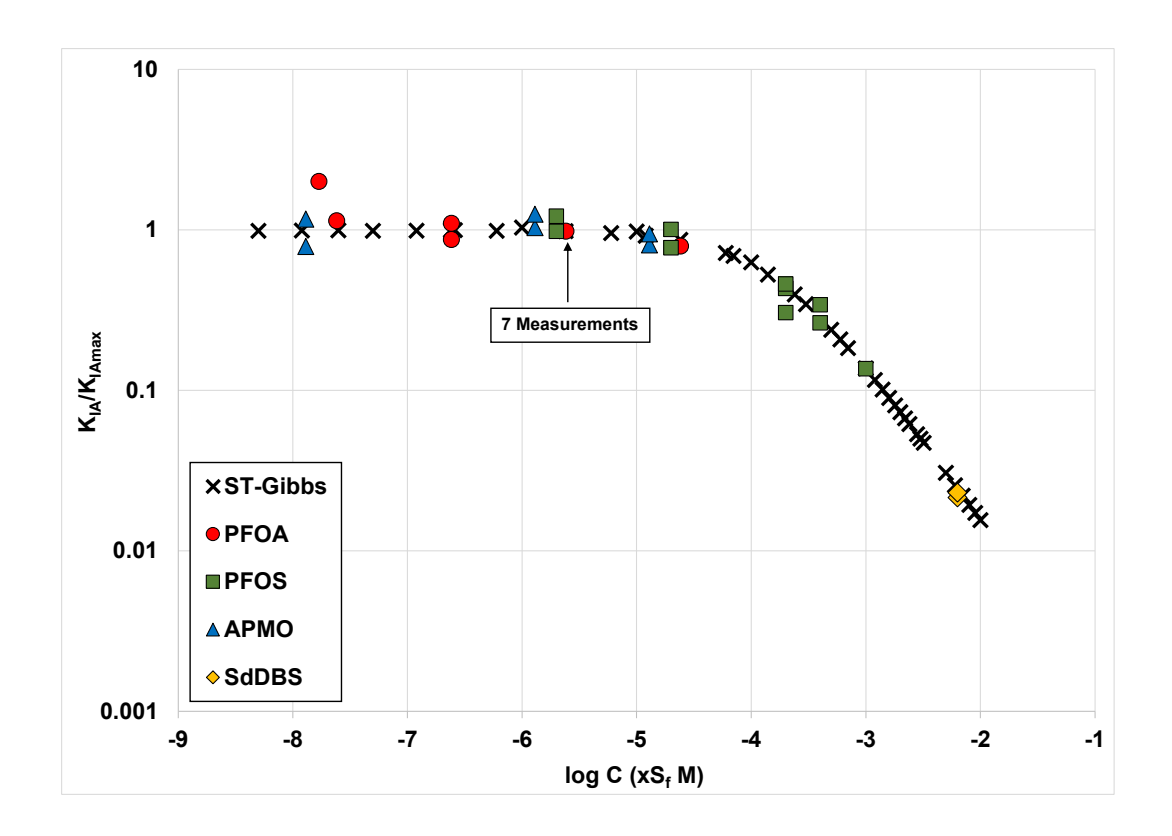


Figure 6. Concentration dependency of K_{IA} values measured from transport experiments. Values are also reported from application of the Gibbs adsorption equation to measured PFOA surfacetension data (ST-Gibbs).

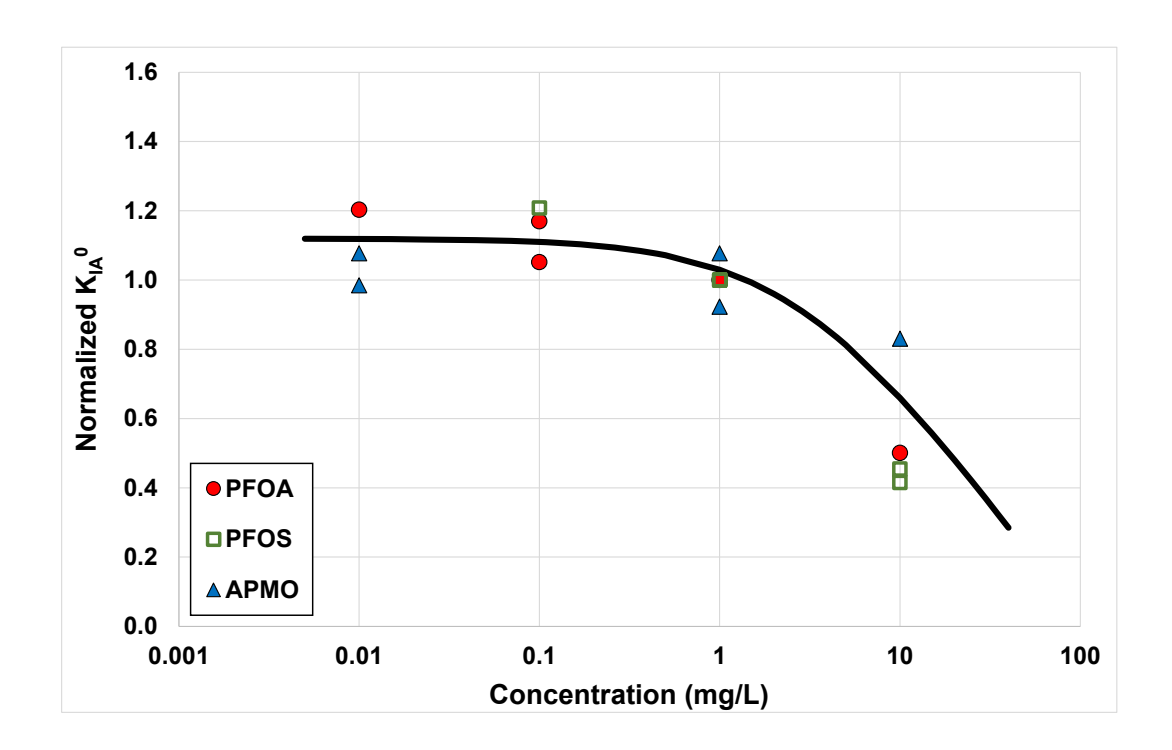


Figure 7. Analysis of concentration dependency of K_{IA}^0 . Note that three and two measurements are represented by the PFOA and PFOS data points, respectively, at C = 1. The line is shown for visualization purposes.

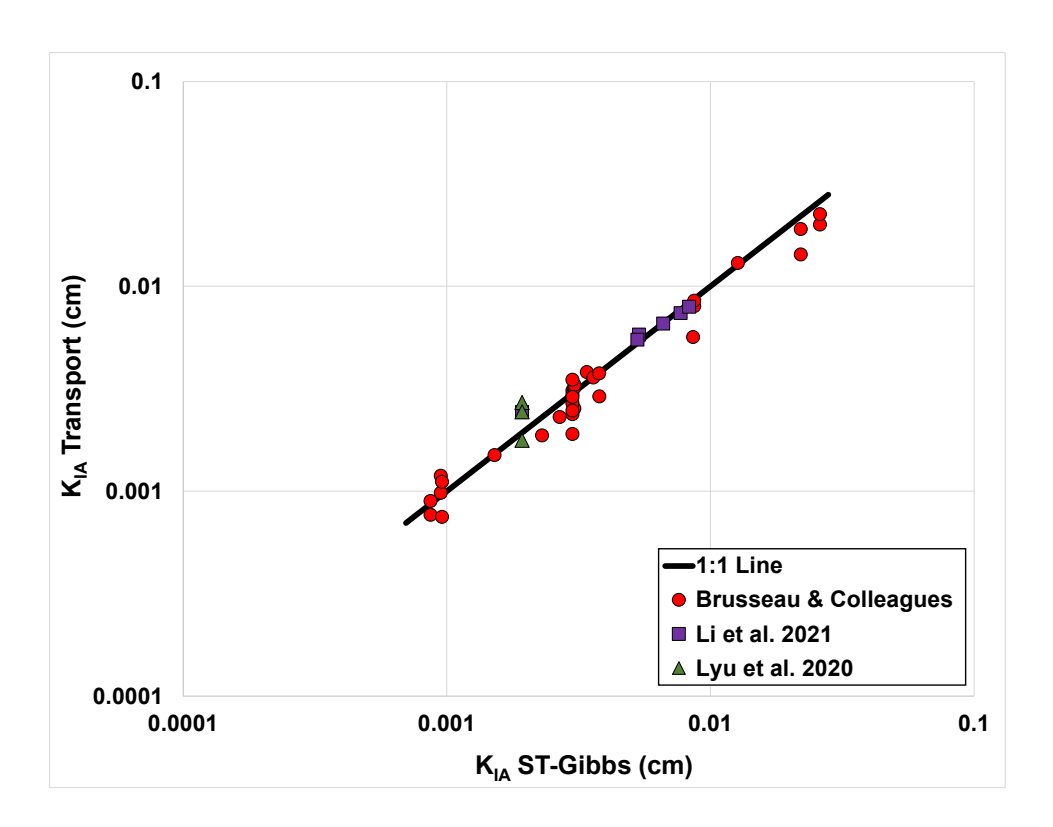


Figure 8. One-to-one comparison of K_{IA} values measured from transport experiments and application of the Gibbs equation to measured surface-tension data.

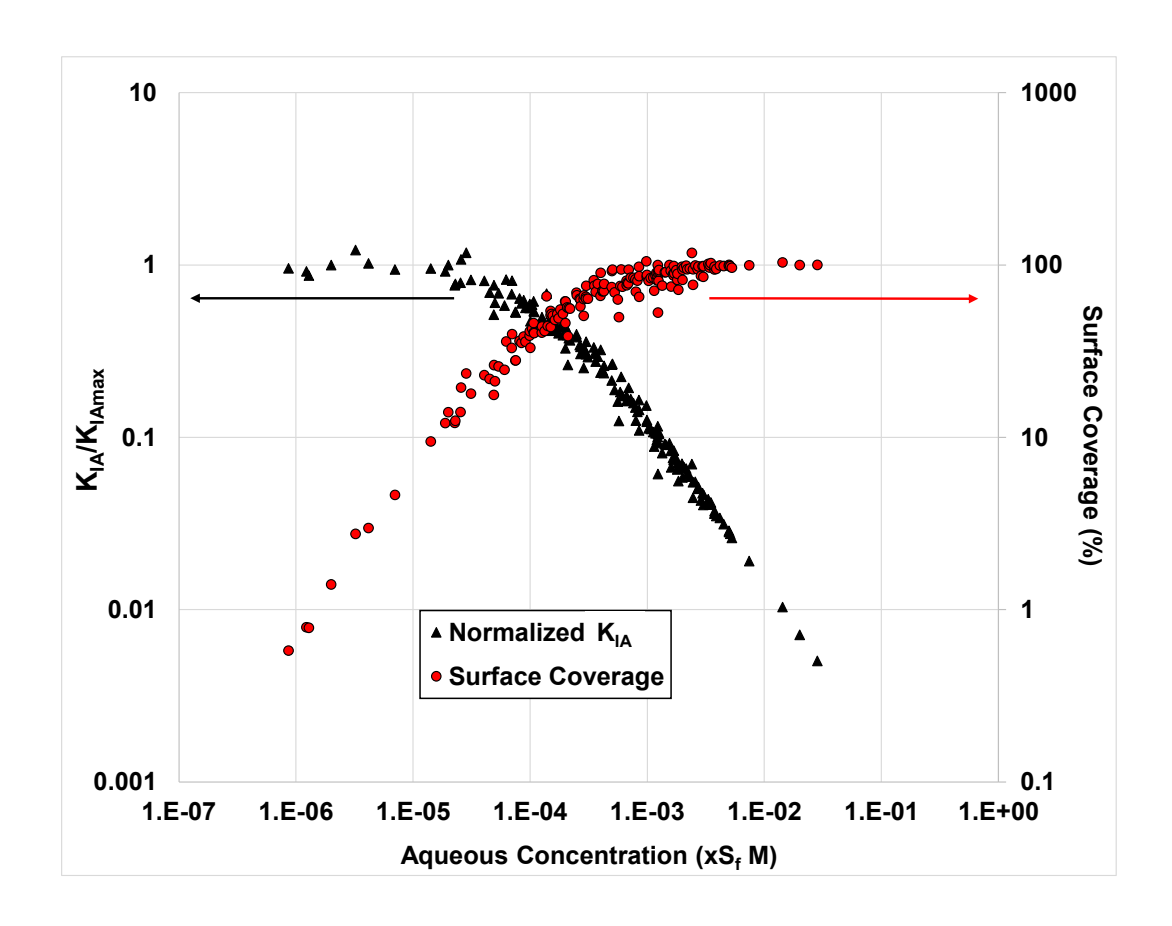


Figure 9. Normalized K_{IA} versus surface coverage (Γ/Γ_{max}) determined from directly-measured data reported in Figures 2A and 3A, respectively.